SCIENCE CHINA
Information Sciences

• RESEARCH PAPER •

June 2018, Vol. 61 062406:1–062406:8
https://doi.org/10.1007/s11432-017-9315-4

Calibration of drift-diffusion model in quasi-ballistic transport region for FinFETs

Lei SHEN, Shaoyan DI, Longxiang YIN, Xiaoyan LIU & Gang DU*

Institute of Microelectronics, Peking University, Beijing 100871*, China*

Received 16 November 2017/Revised 5 December 2017/Accepted 11 December 2017/Published online 14 May 2018

Abstract In the past few years, conventional digital IC technologies have developed rapidly and the device structures have shrunk down to the quasi-ballistic region which strongly affects the device characteristics. The usage of the steady-state transport model and the parameters of the drift-diffusion (DD) method may not correctly model the performance of these devices, including the velocity distributions of the carriers. Several previous studies have suggested modifying the transport parameters of the DD model to continue using it in the quasi-ballistic region. In this paper, a Monte Carlo (MC) simulator is used to calibrate the transport parameters of the DD model for silicon FinFETs. The device features obtained via the parameter-calibrated DD model fit well with the MC simulator. The trends of the calibration factors are also investigated for varying drain voltage, gate voltage, fin width and gate length.

Keywords FinFET, technology computer aided design (TCAD), drift-diffusion, full-band Monte Carlo simulator, quasi-ballistic transport

Citation Shen L, Di S Y, Yin L X, et al. Calibration of drift-diffusion model in quasi-ballistic transport region for FinFETs. Sci China Inf Sci, 2018, 61(6): 062406, https://doi.org/10.1007/s11432-017-9315-4

1 Introduction

As devices scale down to the quasi-ballistic region, the carriers suffer only one or a few scattering events in the channel under a high electric field [1–4]. Quasi-ballistic transport, which strongly affects the device characteristics, has been studied using modeling and simulations [5–14].

The drift-diffusion (DD) model is widely used in technology computer aided design (TCAD) tools due to its efficiency [15]. However, the usage of the steady-state transport model and the parameters of the DD model may not correctly model the performance of devices, including the velocity distributions of the carriers. Early researchers proposed a method using the measured effective carrier velocity, which is a function of the gate voltage instead of the constant saturation velocity [8]. The measurement of the effective velocity is based on experimental data and only devices with gate lengths of approximately 100 nm have been verified. This method cannot be used in simulation studies in the quasi-ballistic region.

By solving the Boltzmann transport equation (BTE) deterministically or using statistical Monte Carlo (MC) methods, the quasi-ballistic transport properties can be more accurately acquired. Devices whose channel materials are silicon or III-V materials have been investigated using BTE solvers [9–12]. However, for present technology nodes, solving the BTE deterministically requires a large amount of computation. Some researchers have coupled the BTE solver in the channel region with the DD equation solver in the

* Corresponding author (email: gangdu@pku.edu.cn)

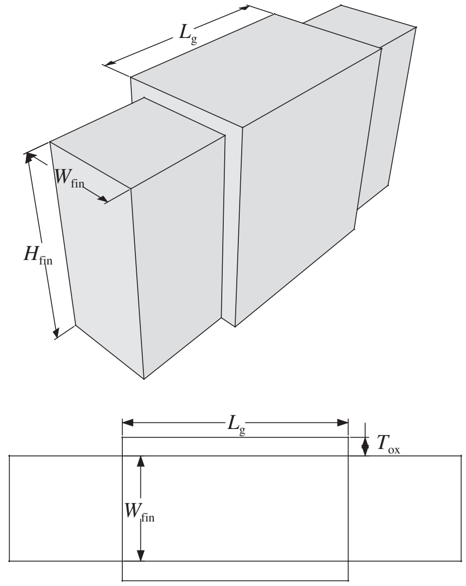

Figure 1 The structure schematics of simulated FinFETs.

source/drain region to obtain the quasi-ballistic transport properties [10]. Nevertheless, this method is still time-consuming and difficult to use directly in industrial research and applications.

The full band Monte Carlo method can investigate the quasi-ballistic transport [16]; however, this is also very time-consuming. Some previous studies have suggested modifying the transport parameters of the DD model to continue using the DD method in the quasi-ballistic region [11, 17, 18]. For III-V materials, the physical models in commercial TCAD tools are not sufficiently mature. Therefore, the calibrations of III-V materials primarily focus on model optimization [11]. Silicon is widely used in scientific research and production, and the models of silicon in commercial TCAD tools are relatively good except for the underestimation in the quasi-ballistic region. Therefore, a fast and accurate calibration procedure is required, especially in industrial production.

In this paper, based on the comparison of the FinFET characteristics in the quasi-ballistic region using the DD and MC methods, a procedure is developed to calibrate the transport parameters of the DD model using the MC simulation results to include the quasi-ballistic transport effect in the DD method.

2 Device and methodology

A 16-nm n-type FinFET, as shown in Figure 1, is simulated using the DD and MC methods. The fin width is 8 nm, and the equivalent oxide thickness is 1 nm. The doping concentrations of the channel and source/drain regions are $10^{16}\mathrm{cm}^{-3}$ and $10^{20}\mathrm{cm}^{-3}$, respectively. Due to the symmetry of FinFETs, a 2D section can be simulated for simplification and efficiency. Sentaurus TCAD [19], which is based on the drift-diffusion transport model and includes low field effective mobility (μ_0), high field saturation model [20], and the Philips unified mobility model [21] ((1)–(7)) was used. The quantum correction and other models were not considered because the focus in this paper is on the calibration of the parameters for the transport properties of the carriers. The parameter-calibrated transport models together with other models can be used to investigate the characteristics of a specific set of devices.

$$\mu\left(F\right)=\frac{\left(\alpha+1\right)\mu_{\mathrm{low}}}{\alpha+\left[1+\left(\frac{(\alpha+1)\mu_{\mathrm{low}}F_{\mathrm{hfs}}}{\nu_{\mathrm{sat}}}\right)^{\beta}\right]^{\frac{1}{\beta}}}, \tag{1}$$

$$v_{\mathrm{sat}}=v_{\mathrm{sat},0}\left(\frac{300K}{T}\right)^{\nu_{\mathrm{sat,exp}}}, \tag{2}$$

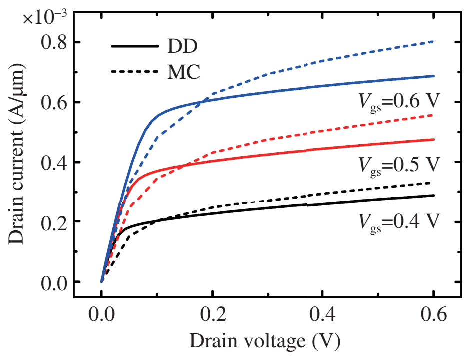

Figure 2 (Color online) The I_{d}-V_{d} curves of 16 nm gate length FinFET obtained from MC and DD.

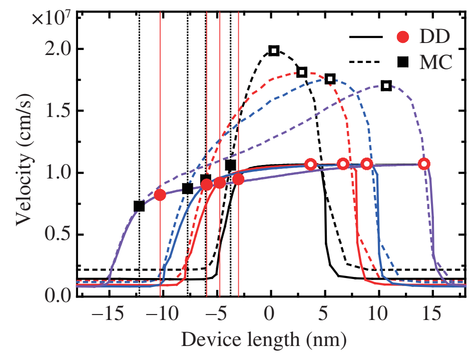

Figure 3 (Color online) The electron velocity distributions obtained via the DD and MC methods with different gate lengths. The solid intersections are the inject velocities and the open symbols are the maximum velocities.

$$\frac{1}{\mu_{i,b}} = \frac{1}{\mu_{i,L}} + \frac{1}{\mu_{i,\mathrm{DAeh}}}, \tag{3}$$

$$\mu_{i,L} = \mu_{i,\max}\left(\frac{T}{300K}\right)^{-\theta_i}, \tag{4}$$

$$\mu_{i,\mathrm{DAeh}} = \mu_{i,N}\left(\frac{N_{i,\mathrm{sc}}}{N_{i,\mathrm{sc,eff}}}\right)\left(\frac{N_{i,\mathrm{ref}}}{N_{i,\mathrm{sc}}}\right)^{\alpha_i} + \mu_{i,c}\left(\frac{n+p}{N_{i,\mathrm{sc,eff}}}\right), \tag{5}$$

$$\mu_{i,N} = \frac{\mu_{i,\max}^2}{\mu_{i,\max}-\mu_{i,\min}}\left(\frac{T}{300K}\right)^{3\alpha_i-1.5}, \tag{6}$$

$$\mu_{i,c} = \frac{\mu_{i,\max}\mu_{i,\min}}{\mu_{i,\max}-\mu_{i,\min}}\left(\frac{300K}{T}\right)^{0.5}. \tag{7}$$

The full-band ensemble Monte Carlo simulator [16, 22–24] including the major scattering mechanisms, such as phonon scattering, impact ionization scattering, and ionized impurity scattering, was used to calibrate the parameters of the DD model.

3 Calibration procedure

The device behaviors in the quasi-ballistic region were studied via a 16-nm gate length FinFET using both the DD and MC methods. The output characteristic curves with different gate voltages are shown in Figure 2. The drain current obtained via the MC method is lower than that obtained via the DD method at a low drain bias. As the drain bias increases, the current obtained via the MC method becomes larger than that obtained via the DD method. When the drain bias and the electric field in the channel become larger, the carriers in the channel suffer fewer scattering events. The original DD model therefore likely underestimates the on-state current.

The obvious difference in the simulation results between the DD and MC methods is the distribution of the electron velocity in the channel, as plotted in Figure 3. The carrier velocity in the channel obtained via the MC method overshoots and is significantly larger than the one obtained via the DD method, which is restricted by the high field saturation model. In the MC simulation, the carriers move in the real and momentum spaces subject to external forces and scattering events. As the electric field increases and the gate length decreases, the carriers are accelerated and the velocity of the carriers is large enough that the carriers can pass through the channel and only suffer a few scattering events. Therefore, the maximum velocity in the channel obtained via the MC method increases when the gate length decreases. In the DD simulation, the velocity saturation model sets a limitation on the maximum velocity. Therefore, the maximum velocities look nearly the same for different gate lengths.

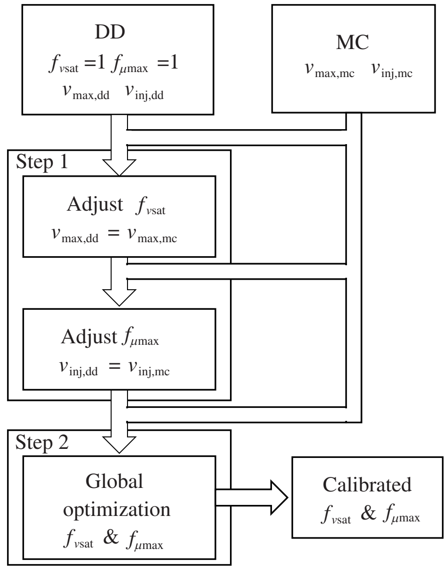

Figure 4 A flow chart of the calibration of the DD model parameters with the MC simulation.

The original DD model needs to be calibrated to be used in the quasi-ballistic region. To achieve an accurate and efficient simulation method, a transport parameter calibration procedure was proposed, as shown in Figure 4. Two target variables ($v_{\rm max}$, $v_{\rm inj}$) and two calibration parameter factors ($f_{v\rm sat}$, $f_{\mu\rm max}$) are considered, where

- $v_{\rm max}$ is the maximum velocity in the channel;
- $v_{\rm inj}$ is the velocity at the top barrier in the channel;
- $f_{v\rm sat}$ is a multiplication factor of the saturation velocity;
- $f_{\mu\rm max}$ is a multiplication factor of $\mu_{\rm max}$ that represents the low-field mobility in the channel in the Philips unified mobility model.

In the DD method, the carrier velocity is limited to a lower value due to the velocity saturation model. By calibrating the saturation velocity (2) of the velocity saturation model in the DD method according to the maximum velocity obtained via the MC method, the carrier velocity in the channel can reach the quasi-ballistic transport state. In the DD method, mobility models are used to reflect the transport characteristics of the channel. The low field mobility ((3)–(7)) is one of the important parameters in the mobility model, which represents the average carrier velocity under a low electric field. In devices with longer gate lengths, the current density can be estimated via the transport mobility, which is acquired via the low field mobility and other factors. The original models and parameters in the DD method could not accurately describe the carrier transport in the quasi-ballistic region. In ballistic theory, the transport properties are represented by the carrier velocity and the charge at the top of the potential barrier. By calibrating the low field mobility of the mobility model in the DD method according to the inject velocity obtained via the MC method, the DD method can be used to approximately simulate the transport characteristics in the quasi-ballistic region.

In step 1, $f_{v\rm sat}$ is first adjusted to match $v_{\rm max,dd}$ with $v_{\rm max,mc}$. Then $f_{\mu\rm max}$ is adjusted to match $v_{\rm inj,dd}$ with $v_{\rm inj,mc}$ using the selected $f_{v\rm sat,s1}$. In step 2, a global optimization is performed to optimize $f_{v\rm sat}$ and $f_{\mu\rm max}$.

A 16-nm gate length FinFET was used to verify the calibration method. First, a set of $f_{v\rm sat}$ from 1.0 to 2.0 was chosen, and the velocity distributions obtained via the DD method are shown in Figure 5. The maximum velocity versus $f_{v\rm sat}$ is plotted in the inset. $f_{v\rm sat,s1}$=1.705 was chosen at the intersection of the inset in Figure 5 to match $v_{\rm max,dd}$ and $v_{\rm max,mc}$. Then, a set of $f_{\mu\rm max}$ from 0.1 to 1.0 with $f_{v\rm sat}$=1.705 was entered into the DD simulation and the velocity distributions were obtained via the DD method as shown in Figure 6. The injection velocities versus $f_{\mu\rm max}$ are plotted in the inset, and $f_{\mu\rm max,s1}$=0.176 is chosen to match the $v_{\rm inj,dd}$ and $v_{\rm inj,mc}$. As we can see in Figure 6, $f_{\mu\rm max}$ has some effect on $v_{\rm max}$; therefore, a

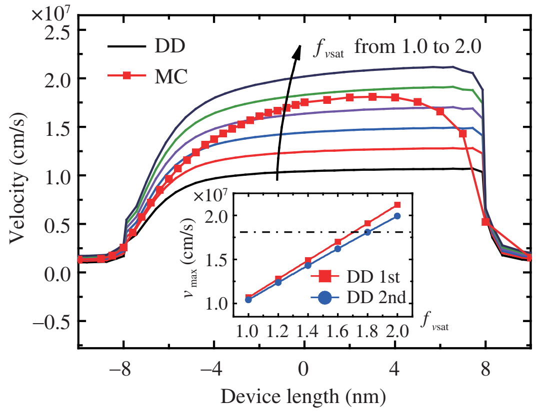

Figure 5 (Color online) The velocity distributions obtained via the MC and DD methods for different $f_{v\mathrm{sat}}$. The $v_{\max}$ obtained via the DD method for different v_{sat} in two steps are shown in the inset (lines with symbols) and the $v_{\max}$ obtained via the MC method is fixed as a horizontal line.

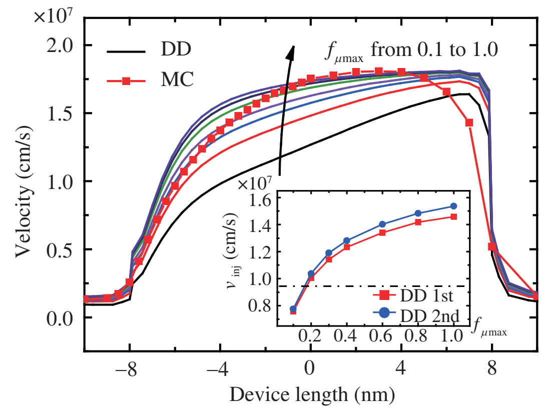

Figure 6 (Color online) The velocity distributions obtained via the MC and DD methods for different $f_{\mu\max}$. The v_{inj} obtained via the DD method for different $\mu_{\max}$ in two steps are shown in the inset (lines with symbols) and the v_{inj} obtained via the MC method is fixed as a horizontal line.

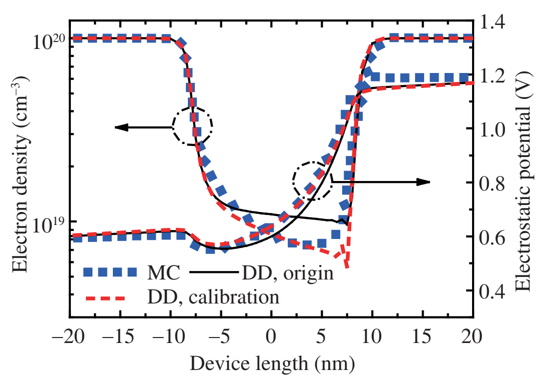

Figure 7 (Color online) The electron density and electric potential distributions obtained via the MC simulation (symbols), the original DD simulation (line), and the calibrated DD simulation (dash line) at $V_{\mathrm{ds}} = V_{\mathrm{gs}} = 0.6$ V.

global optimization is necessary. The adjustment of $f_{v\mathrm{sat,s2}}$ in step 2 uses $f_{\mu\max,\mathrm{s1}}$ instead of 1.0, followed by the calibration of $f_{\mu\max,\mathrm{s2}}$. Then, the final calibration factors $f_{v\mathrm{sat,s2}}$=1.803 and $f_{\mu\max,\mathrm{s2}}$=0.165 are obtained.

4 Results and discussion

As shown in Figure 7, the distributions of the electron density and the electric potential obtained via the parameter-calibrated DD model are closer to the MC method than to the original DD method. Therefore, the parameter-calibrated DD model can be used to approximately simulate the device properties in the quasi-ballistic region.

The tendencies of the inject velocity and the maximum velocity with varying gate length and fin width are plotted in Figures 8 and 9, respectively. The inject velocity obtained via the MC method is larger than that obtained via the DD method when the gate length is small, and the inject velocity obtained via the MC method decreases faster than that obtained via the DD method with increasing gate length. The maximum velocity obtained via the MC method increased when the gate length decreased, while the maximum velocity obtained via the DD method looks nearly the same at different gate lengths. The variations in the target variables with fin width are not obvious because the surface roughness scattering was not considered in this study.

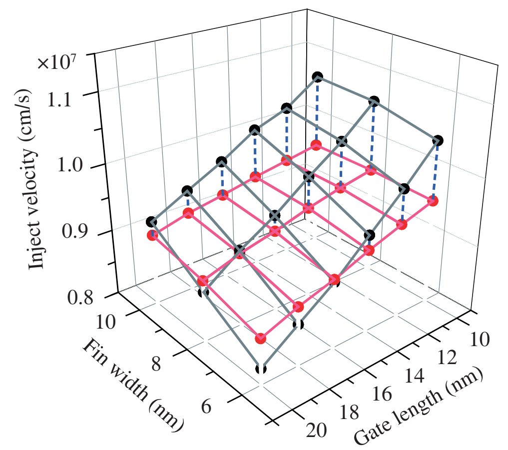

Figure 8 (Color online) The inject velocity for different gate lengths and fin widths obtained via the DD (red) and MC (black) methods.

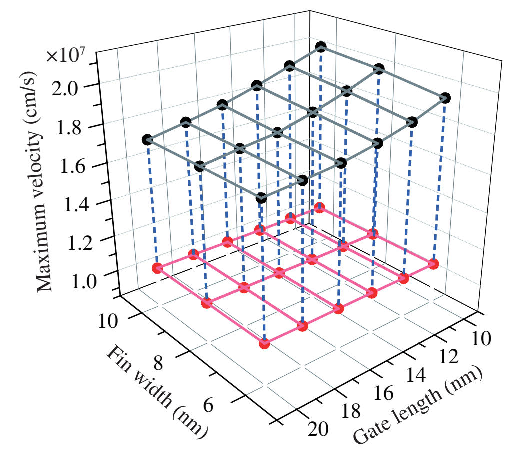

Figure 9 (Color online) The maximum velocity for different gate lengths and fin widths obtained via the DD (red) and MC (black) methods.

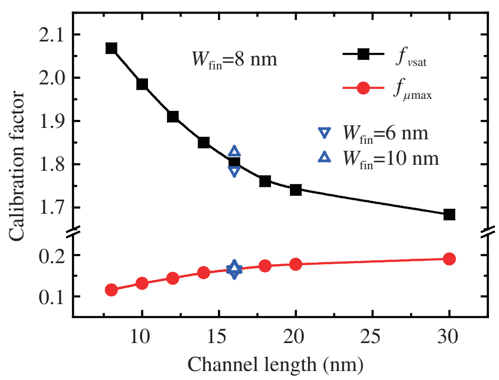

Figure 10 (Color online) Gate length dependencies of the calibration parameters $f_{v\text{sat}}$ and $f_{\mu\text{max}}$ obtained via the calibration procedure.

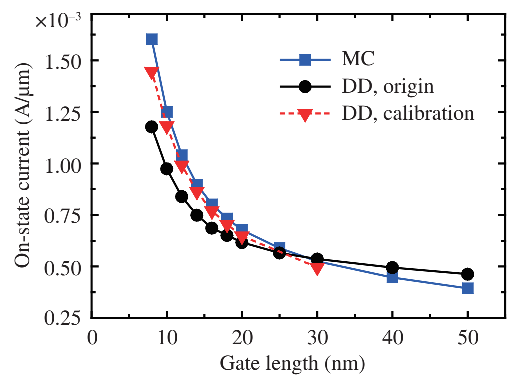

Figure 11 (Color online) The on-state current for different gate lengths obtained via the MC simulations (squares) and DD simulations (circles) at $V_{\rm ds} = V_{\rm gs}$=0.6 V. The calibrated DD simulation results (triangle, dashed line) are also plotted.

The calibration procedure was applied to devices with different gate lengths. The gate length dependencies of the calibration factors are shown in Figure 10. As the gate length decreased, the saturation velocity increased while the low-field mobility was reduced, which is closer to the characteristics of quasi-ballistic transport. The fin width dependencies of the calibration factors with a 16-nm gate length are shown in Figure 10 with triangle markers, and the difference is not obvious.

The on-state current for different gate lengths is shown in Figure 11. The current value obtained via the MC method is larger than that obtained via the DD method when the gate length is small, while a large gate length has the opposite trend. The current obtained via the parameter-calibrated DD method at the lower gate length increases and is much closer to that obtained via the MC method.

To employ the model parameter calibration progress, the calibrated parameters need to be tolerant of the bias conditions. Then, the calibrated DD model can be used to study the output and transfer characteristics of a given device because the model parameters are not easy to calibrate and modify simultaneously with the changing bias.

Figures 12 and 13 show the variation in the inject velocity and maximum velocity with respect to the drain and gate voltages. As the drain voltage decreases, the electric field in the channel decreases and the average velocity that carriers may reach is decreased. At the low electric field, the carrier velocity is

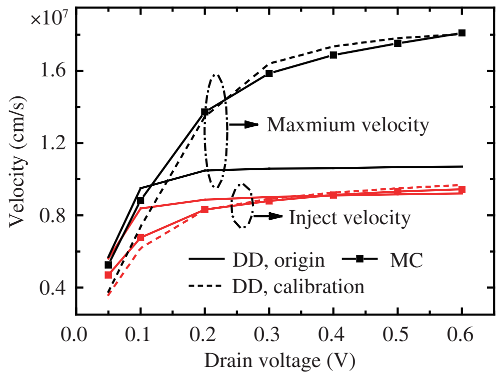

Figure 12 (Color online) The inject velocity and maximum velocity for different drain voltages obtained via the DD (original and calibrated) and MC methods.

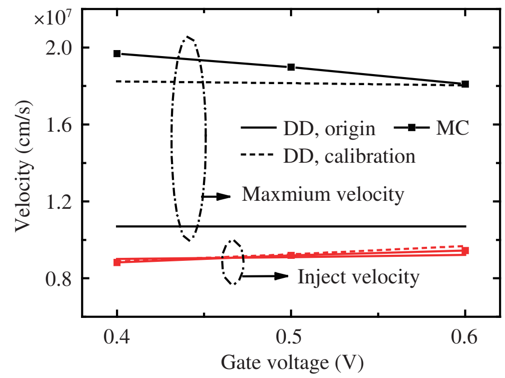

Figure 13 (Color online) The inject velocity and maximum velocity for different gate voltages obtained via the DD (original and calibrated) and MC methods.

lower than the saturation velocity of the velocity saturation model in the DD method and the maximum velocity decreases. Therefore, the maximum velocity obtained via the original DD method remains the same at the high drain voltage and decreases at low drain voltage. The maximum velocity obtained via the MC method increases as the drain voltage increases and is not limited by the velocity saturation model. By calibrating the parameters in the DD method at the on-state, the maximum velocity can exceed the limit as the drain voltage increases. However, due to the tradeoff between the maximum velocity and the inject velocity, the low field mobility is reduced at high drain voltage. Then, the maximum velocity obtained via the calibrated DD method at low drain voltage is slightly lower than that obtained via the MC method and the original DD method. In the original DD method, the distribution of the velocity remains consistent with different voltages and the tendencies of the maximum velocity and the inject velocity at different voltages are similar. In the parameter-calibrated DD method, the inject velocity slightly increases at high drain voltage and decreases at low drain voltage compared to the original DD method, which is closer to the MC method.

The influence of the gate voltage on the maximum velocity and inject velocity is not obvious. The maximum velocity obtained via the MC method slightly decreases when the gate voltage increases. This may be induced by the gradually enhanced carrier-carrier scattering in the channel. The difference in the current in Figure 2 between several gate voltages is due to the different carrier densities in the channel. Therefore, the calibrated parameters of the DD method in the on-state can be used within a certain range of drain and gate voltages.

5 Conclusion

FinFET transistors in the quasi-ballistic region are studied using both DD and MC methods. The DD method is quicker and more efficient; however, the MC method may represent the quasi-ballistic characteristics well. A two-step calibration procedure was therefore introduced. The parameter-calibrated DD method is more accurate than the original model and more efficient than the MC method. The device features obtained via the parameter-calibrated DD model fit well with those obtained via the MC simulator. The calibrated parameters of the DD method in the on-state can be used within a certain range of drain and gate voltages. The trends of the calibration factors were also investigated for varying fin widths and gate lengths.

Acknowledgements This work was supported in part by National Key Research and Development Plan (Grant No. 2016YFA0202101), National Natural Science Fund of China (Grant No. 61421005) and National High Technology Research and Development Program of China (863) (Grant No. 2015AA016501).

References

1 Lundstrom M, Ren Z B. Essential physics of carrier transport in nanoscale MOSFETs. IEEE Trans Electron Dev, 2002, 49: 133–141

2 Rahman A, Guo J, Datta S, et al. Theory of ballistic nanotransistors. IEEE Trans Electron Dev, 2003, 50: 1853–1864

3 Deleonibus S. Looking into the future of Nanoelectronics in the Diversification Efficient Era. Sci China Inf Sci, 2016, 59: 061401

4 Cheng K G, Khakifirooz A. Fully depleted SOI (FDSOI) technology. Sci China Inf Sci, 2016, 59: 061402

5 Natori K. Ballistic metal-oxide-semiconductor field effect transistor. J Appl Phys, 1994, 76: 4879–4890

6 Natori K. Scaling limit of the MOS transistor: a ballistic MOSFET. IEICE Trans Electron, 2001, E84C: 1029–1036

7 Lundstrom M. Elementary scattering theory of the Si MOSFET. IEEE Electron Dev Lett, 1997, 18: 361–363

8 Yang P Z, Lau W S, Ho V, et al. A comparison between the quasi-ballistic transport model and the conventional velocity saturation model for sub-0.1-μm mos transistors. In: Proceedings of Electron Devices and Solid-State Circuits, Taiwan, 2007. 99–102

9 Jin S, Fischetti M V, Tang T W. Theoretical study of carrier transport in silicon nanowire transistors based on the multisubband Boltzmann transport equation. IEEE Trans Electron Dev, 2008, 55: 2886–2897

10 Jin S, Hong S M, Choi W, et al. Coupled drift-diffusion (DD) and multi-subband Boltzmann transport equation (MSBTE) solver for 3D multi-gate transistors. In: Proceedings of IEEE International Conference on Simulation of Semiconductor Processes and Devices, Glasgow, 2013. 348–351

11 Bhuwalka K K, Wu Z, Noh H K, et al. In0.53Ga0.47As-based nMOSFET design for low standby power applications. IEEE Trans Electron Dev, 2015, 62: 2816–2823

12 Di S Y, Shen L, Chang P Y, et al. Performance comparison of Si, III-V double-gate n-type MOSFETs by deterministic Boltzmann transport equation solver. Jpn J Appl Phys, 2017, 56: 04CD08

13 Chang P Y, Liu X Y, Di S Y, et al. Evaluation of ballistic transport in III-V-based p-Channel MOSFETs. IEEE Trans Electron Dev, 2017, 64: 1053–1059

14 Yin L X, Shen L, Di S Y, et al. Investigation of thermal effects on FinFETs in the quasi-ballistic regime. In: Proceedings of International Conference on Solid State Devices and Materials, Sendai, 2017. 241–242

15 Roosbroeck W V. Theory of the flow of electrons and holes in germanium and other semiconductors. Bell Syst Tech J, 1950, 29: 560–607

16 Du G, Liu X Y, Han R Q. Quantum Boltzmann equation solved by Monte Carlo method for nano-scale semiconductor devices simulation. Chin Phys, 2006, 15: 177–181

17 Lundstrom M. Drift-diffusion and computational electronics—still going strong after 40 years! In: Proceedings of International Conference on Simulation of Semiconductor Processes and Devices, Washington, 2015. 1–3

18 Jin S, Pham A-T, Choi W, et al. Performance evaluation of FinFETs: from multisubband BTE to DD calibration. In: Proceedings of International Conference on Simulation of Semiconductor Processes and Devices, Nuremberg, 2016. 109–115

19 Synopsys. Sentaurus TCAD User's Manual, H-2013.03, 2013

20 Canali C, Majni G, Minder R, et al. Electron and hole drift velocity measurements in silicon and their empirical relation to electric field and temperature. IEEE Trans Electron Dev, 1975, 22: 1045–1047

21 Klaassen D B M. A unified mobility model for device simulation-I. Model equations and concentration dependence. Solid-State Electron, 1992, 35: 953–959

22 Du G, Liu X Y, Xia Z L, et al. Monte Carlo simulation of p- and n-channel GOI MOSFETs by solving the quantum Boltzmann equation. IEEE Trans Electron Dev, 2005, 52: 2258–2264

23 Du G, Liu X Y, Xia Z L, et al. Simulation of Si and Ge UTB MOSFETs using Monte Carlo method based on the quantum Boltzmann equation. In: Proceedings of International Workshop on Computational Electronics, West Lafayette, 2004. 186–187

24 Du G, Zhang W, Wang J C, et al. Study of 20 nm bulk FINFET by using 3D full band Monte Carlo method with Effective Potential Quantum Correction. In: Proceedings of IEEE International Conference on Solid-State and Integrated Circuit Technology, Shanghai, 2010. 1952–1954